

Catchment-Scale Flood Hazard Mapping in the Lower Areas of Lam Pao River Basin, Thailand

Worapong Lohpaisankrit^{1,2*} and Haris Prasanchum²

¹Department of Civil Engineering, Faculty of Engineering, Khon Kaen University, Khon Kaen, Thailand

²Department of Civil Engineering, Faculty of Engineering, Rajamangala University of Technology Isan, Khon Kaen, Thailand

woralo@kku.ac.th* and haris.pr@rmuti.ac.th

Abstract. Floods have resulted in the reduction of agricultural production in Thailand. Flood hazard mapping in the lower part of Lam Pao River Basin is a challenging task because its upper part is controlled by the Lam Pao Reservoir. The present study aims at developing flood hazard maps using an integrated approach based on the SWAT hydrological model and satellite data. The SWAT model was used to transform observed daily meteorological data between 2008 and 2017 into runoff hydrographs. The results indicated that the SWAT model had capability to reproduce extreme flood hydrographs according to Nash-Sutcliffe Efficiency, R^2 and percent error in peak. The simulated discharges were found to be satisfactorily fitted to the Gumbel distribution based on the Chi-square test. The flood peaks with return periods of 5, 10 and 20 years at each sub-catchment were classified into four levels of flood hazards, namely low, medium, high and very high flood hazards based on the frequency of flood occurrences acquired from the satellite data. It was found that six sub-catchments along the main river had very high degrees of flood hazard. The results of the sub-catchments S15 and S16 located downstream were verified by the satellite data. There were three flood events occurred in the two sub-catchments during the study period. Moreover, some sub-catchments of tributary streams were found to have high degrees of flood hazard. We conclude that flooding spatial information of satellite data can help to improve hydrological prediction and to prioritise flood protection areas in ungauged sites.

Received by 24 November 2021
 Revised by 18 December 2021
 Accepted by 21 December 2021

Keywords:

Flood frequency, Gumbel distribution, Flood hazard assessment, Return period, SWAT

1. Introduction

Floods are the most widespread of all natural disasters that can happen in many parts of the world. They have not only a negative impact to the environment itself, but can also lead to impacts on society and economic prosperity of

countries [1]. A classical solution for flood control and mitigation has been based on structural measures such as dams, weirs and other river structures. However, this classical solution may not suitable for the present circumstance since land demand for food production and habitat has increased and environmental concern has been increasing. Consequently, several solutions on the basis of non-structural measures have been widely developed and applied for flood control and mitigation. For example, [2] applied statistical procedures in Analytic Hierarchy Process for producing flood hazard, exposure, vulnerability and risk maps, which can be decision support tools for flood management. Such maps can be useful information for maintaining flood awareness and preparedness in local communities.

Over the past few decades, hydrological models have been involved in disaster management. One of widely used hydrological models is the Soil and Water Assessment Tool (SWAT) model. This model is a semi-distributed basin-scale model that creates hydrological response units (HRUs) based on the combination of homogeneous topographical, land use and soil characteristics [3]. It has been designed to monitor temporal changes of surface runoff in response to land use changes [4]. In addition, the model can be used to assess changes in hydrological extremes in response to climate change. Therefore, outcomes (e.g. peak flood discharge) computed by the hydrological models can be useful information for evaluating the exceedance probabilities for extreme hydrological events [5, 6].

Flood hazard mapping is a necessary component in flood mitigation and management. Degrees of flood hazard in a map can be presented by using a simple classification such as indicating very high, high, moderate and low hazard [7]. Flood hazard mapping usually requires data of flood inundation areas, which can be obtained using remote sensing techniques or generated using combined hydrological and hydraulic modelling approaches [8, 9].

The lower areas of the Lam Pao River Basin have been flooded for weeks during the rainy season [10]. The floods mainly cause damage to agricultural production. These floods are highly unpredictable because they can happen as consequent upon heavy releases from the dam and intense

rainfall in the areas. Thus, the assessment of flood hazard is necessary in order to establish and implement appropriate flood mitigation measures in the river basin.

The main objective of this study is to assess the flood hazard in the lower areas of Lam Pao River Basin by integrating outcomes of the hydrological SWAT model and remotely sensed data of flood events. Results of flood hazard assessment are interpreted through catchment-scale maps. These maps can be used to identify areas having been affected by floods and high levels of flood hazard. Therefore, the flood hazard maps may be useful information in prioritising the areas for flood mitigation plan.

2. Materials and Methods

2.1 Study Area and Data

The setting for this study was a part of the Lower Lam Pao River Basin located downstream of Lam Pao Dam covering Kalasin and Maha Sarakham Provinces. One of the main objectives of the dam is flood prevention. However, floods frequently occur in the lower part of the basin and cause damage to many sectors, especially agriculture. Specifically, the areas of approximately 1,180 km² from Lam Pao Dam downstream to the E.87 stream

gauging station was considered as the study catchment (Fig. 1). The elevation of this catchment ranges from 131 to 233 m a.s.l. (average 157 m).

According to 11-year data (2007-2017) recorded in the five rainfall stations of the Thai Meteorological Department (Fig. 1), average annual rainfall is 1,343 mm, with maxima in rainy season (from May to October). In addition to the rainfall data, other meteorological data, namely maximum and minimum air temperature, wind speed, relative humidity and solar radiation, were collected at the Kamalasai meteorological station. The inflow to the catchment is controlled by Lam Pao Dam and monitored at the E.75 stream gauging station. Therefore, runoff data used in this study were collected at the E.75 and E.87 stations from Royal Irrigation Department.

Spatial data used in this study consisted of digital elevation model (DEM) with 30 m resolution, while land use and land cover (LULC) and soil type data were obtained from Land Development Department. The LULC and soil type data were available at a scale of 1:50,000. According to the historical LULC data in 2015, the predominant LULC was rice paddy (Fig. 2a). The study catchment was mainly formed by sandy loam and loam on the basis of the soil type data observed in 2015 (Fig. 2b).

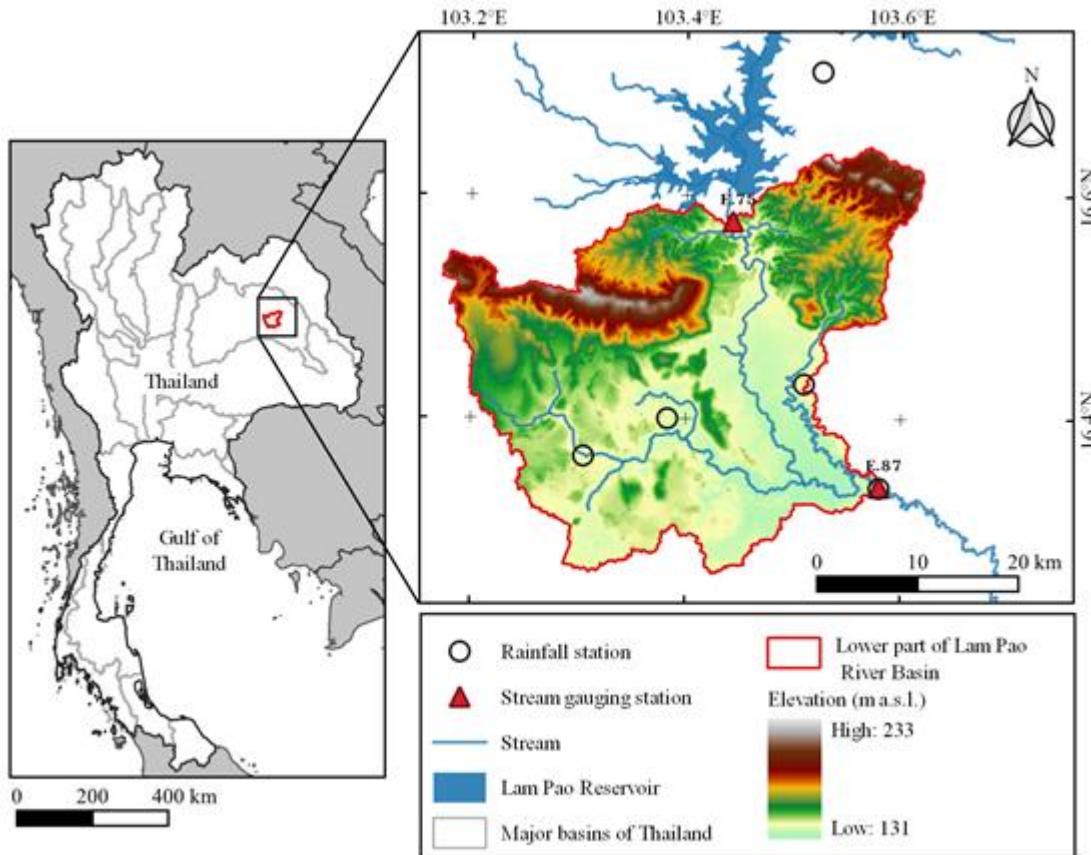


Fig. 1 Location of rainfall and stream gauging stations used in this study

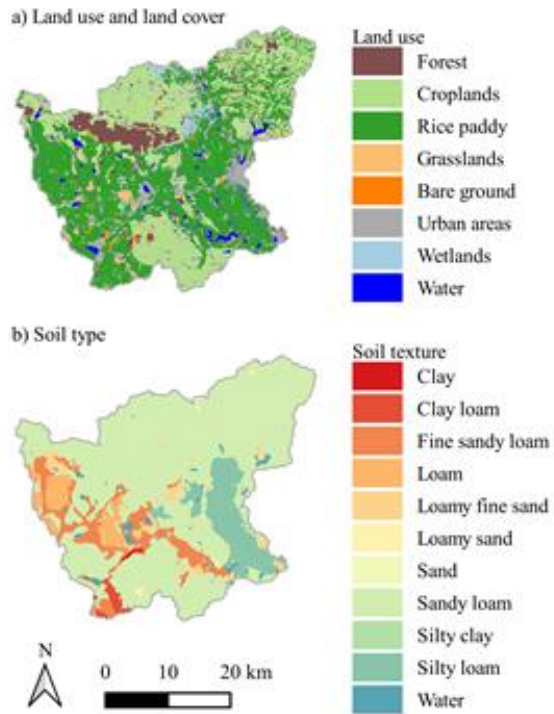


Fig. 2 Spatial data of study area: a) land use and land cover map and b) soil type map

2.2 Estimation of Peak Runoff Rates

Owing to lack of runoff information available at sub-catchment scales, a hydrological modelling-based approach was introduced to transform from rainfall and meteorological data into runoff. In this approach, the semi-distributed hydrological SWAT model was applied to estimate peak runoff rates at a sub-catchment level in the lower areas of Lam Pao River Basin because this model has been successful in simulating runoff in various environmental watersheds [11]. Sub-catchments of the basin were delineated from the DEM by using QSWAT 1.9 tools. In addition, physical characteristics of the sub-catchments were computed based on the DEM, LULC and soil datasets. Three of the physical characteristics, which were slopes, LULC types and soils, were used to form hydrological response units (HRUs) in the sub-catchments. Each HRU has a unique composition of those three characteristics [1]. On the basis of the datasets, the study area was divided into 17 sub-catchments and 260 HRUs.

Since the study area is not a headwater watershed, its upper boundary condition was controlled by runoff from Lam Pao Dam. The runoff released from the dam has been recorded at the E.75 station. Therefore, these runoff data were assigned as inflow to sub-catchment S12 of the SWAT model, which was located at the top of the study catchment. Moreover, the meteorological data, namely daily rainfall, air temperature, wind speed, relative humidity and solar radiation from 2007 to 2017 were input into the model.

In this study, there were three modelling periods. The period of 2007 was firstly considered as a model warm-up period. As a result, initial hydrological conditions of the study catchment were generated by the SWAT model. The periods of 2008-2012 and 2013-2017 were model calibration and validation, respectively. After the warm-up period, the SWAT model was used to transform the daily meteorological data to daily runoff data. These data were then compared with observed runoff data at the E.87 station at the same periods. The calibration and validation processes were accomplished when reasonable results of model simulation based on statistical indices such as the Nash-Sutcliffe Efficiency coefficient (NSE), coefficient of determination (R^2) and percent error in peak (PEP) were obtained.

2.3 Evaluation of Model Performance

As aforementioned, during the calibration and validation processes, the model performance was achieved based on NSE, R^2 and PEP. NSE provides a normalised statistic indicating how well the simulated outcomes match the observed data. NSE ranges between $-\infty$ and 1, with a value equal to 1 being the optimal value. The coefficient of determination (R^2), which ranges between 0 and 1, describes the degree of collinearity between simulated and observed data. Typically, the model performance is considered acceptable when values of NSE and R^2 are greater than 0.5 for a daily time step simulation [12]. PEP is an important statistical index in flood studies. It measures the relative error of peak value comparing to the observed peak value. The model is considered satisfactory when the absolute value of PEP less than 20% [Yu]. The statistical indices are defined in the following equations:

$$NSE = 1 - \frac{\sum_{i=1}^n (Q_s(i) - Q_o(i))^2}{\sum_{i=1}^n (Q_o(i) - \bar{Q}_o)^2}, \quad (1)$$

$$R^2 = \frac{[\sum_{i=1}^n (Q_o(i) - \bar{Q}_o)(Q_s(i) - \bar{Q}_s)]^2}{[\sum_{i=1}^n (Q_o(i) - \bar{Q}_o)^2][\sum_{i=1}^n (Q_s(i) - \bar{Q}_s)^2]}, \quad (2)$$

$$PEP = \frac{(Q_{o,peak} - Q_{s,peak})}{Q_{o,peak}} \times 100\%, \quad (3)$$

where NSE is the Nash-Sutcliffe Efficiency coefficient, R^2 is the coefficient of determination, PEP is the percent error in peak, n is the total number of observations, $Q_s(i)$ is the i^{th} simulated runoff ($\text{m}^3 \text{s}^{-1}$), $Q_o(i)$ is the i^{th} observed runoff ($\text{m}^3 \text{s}^{-1}$), Q_s and Q_o are the average values of the simulated and observed runoff ($\text{m}^3 \text{s}^{-1}$), respectively, and $Q_{s,peak}$ and $Q_{o,peak}$ are the peak values of the simulated and observed runoff ($\text{m}^3 \text{s}^{-1}$), respectively.

2.4 Determination of Peak Flood Frequency

In the present study, Gumbel distribution was applied to analyse the series of annual maximum daily (AMD) discharges for the 10-year observations since it is considered applicable for areas with short-term records of discharges [14]. However, the Gumbel distribution was examined whether it was suitable for the AMD discharges of the 17 sub-catchments simulated by the SWAT model. There were two main procedures: 1) estimation of maximum discharges in different return periods and 2) assessment of the goodness of fit of the Gumbel distribution.

The estimation of maximum discharges was based on the method of moments [15]. The moments of the data series such as its mean and standard deviation were computed. Afterwards, the maximum discharge corresponding to a return period (T_r) can be estimated as in Eq. (4).

$$Q_{Tr} = Q_{mean} + KS_Q, \quad (4)$$

where Q_{Tr} is the maximum discharge corresponding to a return period (T_r), Q_{mean} is the mean of the data series (i.e. maximum discharge), S_Q is the standard deviation of the data series and K is the frequency factor.

According to [16], the frequency factor of the Gumbel distribution can be computed as follows:

$$K = -\frac{\sqrt{6}}{\pi} \left\{ 0.5772 + \ln \left[\ln \left(\frac{Tr}{Tr-1} \right) \right] \right\}, \quad (5)$$

where K is the frequency factor of the Gumbel distribution and Tr is the return period.

To assess the goodness of fit between the series of AMD discharges and predicted discharges based on the Gumbel distribution, the Chi-square test was applied. The Chi-square statistic (χ^2) is expressed in Eq. (6) as:

$$\chi^2 = \sum_{i=1}^n (O_i - E_i)^2 / E_i, \quad (6)$$

where n is the number of intervals, O_i is the number of observed discharges (simulated values) in the class interval i and E_i is the number of the corresponding expected values in the class interval i . According to the Chi-square test, the null hypothesis that the series of AMD discharges were distributed as Gumbel distribution at 5% significance level can be accepted for flood frequency and hazard assessment.

2.5 Classification of Flood Hazards

Classification of flood hazards at sub-catchment levels was based on the hydrological modelling approach combined with the satellite remote sensing data, which was the annual flood occurrences analysed by the Geo-Informatics and Space Technology Development Agency (GISTDA) in Thailand.

Maximum daily discharges of the 17 sub-catchments corresponding to a return period such as the 5-, 10- and 20-year return periods were classified into four flood hazard levels (low, medium, high and very high). For flood hazard classification, the range of daily discharge values was obtained by comparing the flood hazard level of each sub-catchment with the number of annual flood occurrences between 2008 and 2017 in the sub-catchment obtained from remote sensing techniques. Based on the comparison between the peak discharges and the number of flood occurrences, the peak discharges (Q_{peak}) ranged from 0 to $270 \text{ m}^3 \text{s}^{-1}$ were equally divided into three intervals. Flood hazards were classified as low ($Q_{peak} < 90 \text{ m}^3 \text{s}^{-1}$), medium ($90 \text{ m}^3 \text{s}^{-1} \leq Q_{peak} < 180 \text{ m}^3 \text{s}^{-1}$) and high ($180 \text{ m}^3 \text{s}^{-1} \leq Q_{peak} < 270 \text{ m}^3 \text{s}^{-1}$). If the peak discharges were equal to or greater than $270 \text{ m}^3 \text{s}^{-1}$, flood hazard of sub-catchments was classified as very high in the present study.

3. Results and Discussion

In this section, the results of the hydrological modelling approach are presented in brief. Subsequently, the results of flood hazard mapping are presented in more detail since the main attention of this study was to develop flood hazard maps in areas located downstream of the dam.

3.1 Model Calibration and Validation for Daily Flow Simulation

Model parameters chosen for calibration were based on the sensitivity analysis using the SWAT-CUP program. In the present study, a model parameter with a p-value less than 0.03 was considered to be significantly sensitive to the simulation results. According to 500 simulations of the SWAT-CUP, five parameters, which were initial SCS runoff curve number for moisture condition II (CN2), Soil evaporation compensation factor (ESCO), Manning's n value for the main channel (CH_N2), Groundwater delay (GW_DELAY) and average slope steepness (HRU_SLP), were found to be sensitive because their p-values were smaller than 0.03. Therefore, values of these five parameters were adjusted in the calibration procedure and then were validated by comparing with observed daily discharge series.

Fig. 3 shows the comparisons of simulated and observed hydrographs at the E.87 station for both calibration (2008-2012) and validation (2013-2017) periods. In addition to the visual comparisons, the performance indicators for both periods were considered satisfactory because the values of NSE and R^2 were greater than 0.71 and the absolute values of PEP were less than 20% [12, 13]. The results pointed out that the SWAT model has the ability to reproduce historical flood hydrographs at the E.87 station. Therefore, the SWAT model can be used to simulate daily discharges for the 17 sub-catchments of the drainage area of the E.87 station.

3.2 Flood Hazard Mapping

The AMD discharges of the 17 sub-catchments simulated using the SWAT model were individually frequency analysed. The series of the AMD discharges were found to be satisfactorily fitted to the Gumbel distribution on the basis of the Chi-square test. In this study, the degree of freedom was considered as one for the Gumbel distribution. Therefore, its theoretical value of the Chi-square statistic is 3.84 at 5% significance level. From Table 1, it may be noted that the computed Chi-square values for all sub-catchments are lesser than the theoretical value. This indicated that the Gumbel distribution can be considered acceptable for the flood frequency analysis in the sub-catchments. Thus, this Gumbel distribution can be used to estimate flood magnitude for various return periods, namely 5-, 10- and 20-year return periods.

In addition, Table 1 displays the maximum daily flood discharges estimated using the Gumbel distribution. The maximum daily discharges were increased corresponding to larger return periods. In the present study, the maximum possible flood discharges for return periods up to 20 years were estimated since the annual maximum discharge data were taken from the 10-year observations and satellite-based flood information of about 10 years was available. If the estimation of the maximum daily discharges was extended further, results may be considered undesirable for the statistical analysis of annual maximum discharges [17].

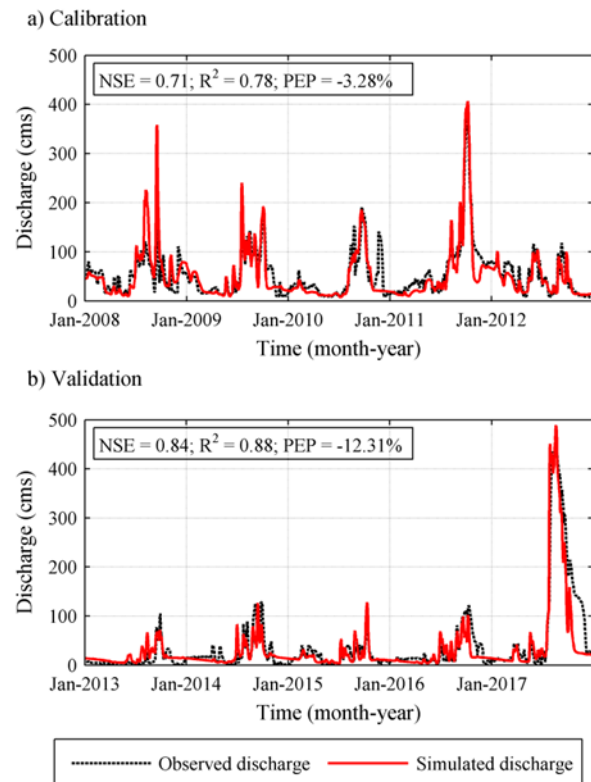


Fig. 3 Calibration and validation

Sub-catchment	Statistical parameters		Chi-square value	Estimated maximum daily discharge ($m^3 s^{-1}$)		
	Mean ($m^3 s^{-1}$)	SD ($m^3 s^{-1}$)		Tr = 5 years	Tr = 10 years	Tr = 20 years
S1	40.6	8.0	0.66	46.4	51.1	55.6
S2	32.1	8.4	0.10	38.1	43.0	47.7
S3	58.2	30.8	1.57	80.4	98.4	115.7
S4	27.2	9.9	0.56	34.3	40.1	45.7
S5	53.5	31.3	1.38	76.0	94.3	111.9
S6	38.4	17.2	0.09	50.8	60.8	70.4
S7	42.3	11.4	0.09	50.6	57.3	63.7
S8	36.1	17.3	0.71	48.6	58.7	68.4
S9	84.4	41.7	0.66	114.4	138.8	162.2
S10	103.5	49.6	0.74	139.1	168.2	196.0
S11	128.2	50.4	0.00	164.5	194.0	222.3
S12	220.9	163.3	2.65	338.3	433.9	525.5
S13	226.9	159.0	2.84	341.3	434.4	523.7
S14	225.6	154.1	2.78	336.5	426.6	513.1
S15	231.1	154.6	2.65	342.3	432.7	519.5
S16	283.4	143.3	1.47	386.5	470.4	550.8
S17	295.2	146.0	0.46	400.2	485.6	567.6

Table 1 Values of Chi-square test and maximum daily discharges for several return periods (Tr) using Gumbel distribution

It can be seen from the data in Table 1 that the sub-catchment S17 had the highest maximum flood discharges of 400.2, 485.6 and $567.6 \text{ m}^3\text{s}^{-1}$ for the return periods of 5, 10 and 20 years, respectively.

Fig. 4a shows the number of years between 2008 and 2017 where floods occurred in the 17 sub-catchments according to satellite remote sensing observations from the GISTDA. For example, there were three years where flood occurrences were observed in the sub-catchment S15 and S16. Moreover, there were two years during the 10-year observations where flood occurrences were reported in the sub-catchment S11 and S17.

To create flood hazard maps, the estimated maximum flood discharges of the 17 sub-catchments were classified into four different hazard levels (very high, high, medium and low) and compared with the annual flood occurrences observed by the GISTDA. Figure 4b presents the flood hazard map of 5-year return period. It was found that the estimated daily maximum flood discharges in the sub-catchment S12, S13, S14, S15, S16 and S17 were greater than $270 \text{ m}^3\text{s}^{-1}$. As a result, the very high level of flood

hazard was assigned to these sub-catchments for the return period of 5 years. The highest maximum flood discharge found in the sub-catchment S17 was relatively greater than the average annual peak flow by about 36%. Moreover, the sub-catchment S9, S10 and S11 fall into the medium level of flood hazard because their estimated daily maximum flood discharges ranged from 90 to $180 \text{ m}^3\text{s}^{-1}$.

Fig. 4c and 4d illustrate flood hazard maps of 10-year and 20-year return periods, respectively. For the both return periods, the results indicated that the sub-catchments with the very high level of flood hazards were the sub-catchments S12, S13, S14, S15, S16 and S17. The results of the sub-catchments S15 and S16 were confirmed by the annual maximum flood maps reported by GISTDA (see Fig. 4a). There were three flood events, which occurred in the two sub-catchments. The sub-catchment S11 can be categorised as a high level of flood hazard because its estimated daily maximum flood discharges for the 20-year return period were between 180 and $270 \text{ m}^3\text{s}^{-1}$. According to the remote sensing observations of flood occurrences,

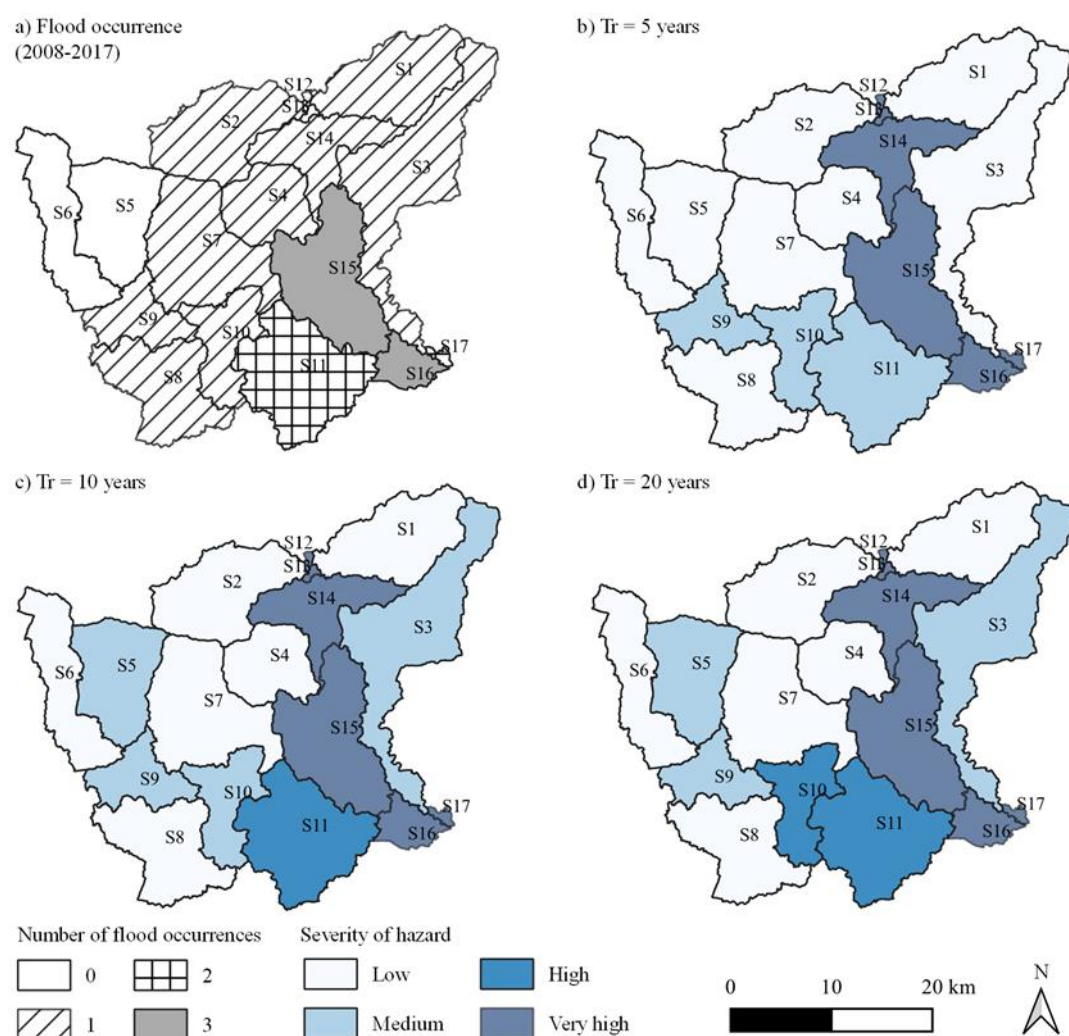


Fig. 4 Maps of flood occurrences and hazard for the lower sub-catchments of the Lam Pao Dam: a) the number of flood occurrences, b) 5-year c) 10-year, and d) 20-year flood hazard sub-catchments

two flood events were observed in the sub-catchment S11 during the 10-year observations (2008-2017). The estimated daily maximum flood discharges of the sub-catchment S10 ranged from 90 to 180 m^3s^{-1} and from 180 to 270 m^3s^{-1} for the return periods of 10 and 20 years, respectively. Therefore, flood hazard levels of this sub-catchment were classified as medium and high for the flood hazard maps of 10-year and 20-year return periods, respectively.

In this paper, a methodology to assess flood hazard on ungauged catchments is presented. A semi-distributed hydrological model was used to simulate the runoff hydrographs of interesting sites. This approach has been found useful for transferring hydrological information from gauged basins to ungauged sites, where runoff information is insufficient for flood modelling and analysis [8, 18]. However, it is important to note that the hydrological model usually does not take into account the capability of river channel. As a consequence, the hydrological model cannot give causes of flooding from overbank flows.

The use of satellite remote sensing observations of flooded areas as an additional data source to support flood hazard assessment was proposed in this study. Remote sensing provides spatial information on flooding areas and its products are cost-effective options for monitoring changes on the Earth surface. Some limitations of the remote sensing observations include inability to detect flood discharges and a coarse temporal resolution of a few days or a few weeks. However, the use of remote sensing observations integrated with outcomes from the hydrological model has potential to improve the assessment of flood hazard, even in ungauged sites. In addition, the present integrated approach could be useful in contributing to similar circumstances, which prioritise areas for flood hazard mitigation.

4. Conclusion and Suggestions

The present study applied hydrological modelling, flood frequency and remote sensing approaches to produce flood hazard maps in order to prioritise sub-catchments located downstream of Lam Pao Dam for flood risk management. The calibration and validation results of the SWAT model showed good agreement between the observed and simulated discharge data on the basis of the Nash-Sutcliffe Efficiency coefficient, coefficient of determination and percent error in peak. Thus, the SWAT model is considered reasonable for the estimation of discharge at a sub-catchment scale. According to the Chi-square test, annual maximum daily discharges of the sub-catchments were satisfactorily fitted to the Gumbel distribution. Therefore, flood frequency analysis based on the Gumbel distribution was performed in order to determine the exceedance probabilities for floods of any given discharge of the sub-catchments.

In addition, integrating outcomes of the hydrological modelling and flood frequency approaches with the use of remote sensing data has potential to improve the reliability of flood hazard analyses because the spatial extent of floods can be derived from the remote sensing data. In this study, the number of flood occurrences was obtained from remote sensing data. These data were used for assessing the degree of flood hazards. The resultant flood hazard maps for 5-, 10- and 20-year return periods using the hydrological approach revealed that two sub-catchments (i.e., S15 and S16) along the main river and near the outlet of the study area had very high degrees of flood hazard. On the basis of the remote sensing data, three flood events occurred in the sub-catchments between 2008 and 2017.

All in all, an attempt has been made to integrate the particular results of hydrological modelling and remote sensing. Flood probabilities estimated from a hydrological model can be linked to the number of flood occurrences derived by using remote sensing images. One of the main problems of a hydrological modelling-based approach is that simulated runoff amounts accumulate from upstream to downstream areas. As a result, higher levels of flood hazard were found in sub-catchments along the main river. Moreover, the storage capacity of a watercourse is not normally taken into consideration in hydrological modelling. To improve the accuracy and reliability of flood estimates using the hydrological modelling-based approach, information of bankfull discharge at sites of interest should be considered. Some inconsistency in results between hydrological modelling and remote sensing was found. However, the information of flood occurrences obtained from satellite remote sensing observations is considered to be useful for verifying some flood hazard areas determined by the hydrological model. Our suggestion for further improvements of flood hazard mapping is to apply a hydraulic model, which can take account of physical characteristics of river channels. The combination of the hydrological and hydraulic models could be used to generate flood extents and produce a more detailed flood hazard map.

Acknowledgements

The authors would like to thank Khon Kaen University, Thailand and Rajamangala University of Technology Isan, Thailand, for being hubs of this research. Moreover, our sincere appreciation goes to Royal Irrigation Department, Thai Meteorological Department and Land Development Department for supporting the data.

References

- [1] D. Dutta, S. Herath, K. Musiake, "A mathematical model for flood loss estimation," *Journal of Hydrology*, vol. 277, no.1-2, pp. 24–49, 2003. DOI: 10.1016/S0022-1694(03)00084-2.
- [2] C. Luu, J. Meding, "A Flood Risk Assessment of Quang Nam, Vietnam Using Spatial Multicriteria Decision Analysis," *Water* vol.10, no.4, pp.461, 2018. DOI: 10.3390/w10040461.

- [3] J.G. Arnold, D.N. Moriasi and et.al, "SWAT: model use, calibration, and validation," *Trans. ASABE*, vol.55, no.4, pp.1491–1508, 2012. DOI: 10.13031/2013.42256.
- [4] H. Prasanchum, A. Kangrang, R. Hormwichian, "Change in Inflow and Hydrologic Response Due to Proactive Agriculture Land Use Policy in Northeast of Thailand," *International Review of Civil Engineering*, vol.11, no.3, pp.141, 2020. DOI: 10.15866/irece.v11i3.18240.
- [5] M. Iqbal, Z. Dahri, E. Querner, A. Khan, N. Hofstra, "Impact of Climate Change on Flood Frequency and Intensity in the Kabul River Basin," *Geosciences*, vol.8, no.4, pp.114, 2018. DOI: 10.3390/geosciences8040114.
- [6] W. Lohpaisankrit, T. Hiranwattananon, N. Tumma, "Application of a rainfall-runoff model for flood generation in the Huai Sangka catchment, Thailand," *Engineering and Applied Science Research*, vol.48, no.2, pp.121–130, 2021. DOI: 10.14456/easr.2021.14.
- [7] T. Tingsanchali and F. Karim, "Flood-hazard assessment and risk-based zoning of a tropical flood plain: case study of the Yom River, Thailand," *Hydrological Sciences Journal*, vol.55, no.2, pp.145–161, 2010. DOI: 10.1080/02626660903545987.
- [8] M. Z. Khaing, K. Zhang, H. Sawano, B. B. Shrestha, T. Sayama, K. Nakamura, "Flood hazard mapping and assessment in data-scarce Nyaungdon area, Myanmar," *PLoS One* 14, e0224558, 2019. DOI: 10.1371/journal.pone.0224558.
- [9] W. Lohpaisankrit, G. Meon, T. Tingsanchali, "A framework of integrated hydrological and hydrodynamic models using synthetic rainfall for flash flood hazard mapping of ungauged catchments in tropical zones," *Proc. IAHS*, vol.373, pp.183–187, 2016. DOI: 10.5194/iahs-373-183-2016.
- [10] N. Arunyanart, C. Limsiri, A. Uchaipichat, "Flood hazards in the Chi River Basin, Thailand: Impact management of climate change," *Applied Ecology and Environmental Research*, vol.15, no.4, pp.841–861, 2017. DOI: 10.15666/aeer/1504_841861.
- [11] W. P. Gassman, R. M. Reyes, H. C. Green, G. J. Arnold, "The soil and water assessment tool: historical development, applications, and future research directions," *Transactions of the ASABE*, vol.50, no.4, pp.1211–1250, 2007. DOI: 10.13031/2013.23637.
- [12] N. D. Moriasi, W. M. Gitau, N. Pai and P. Daggupati, "Hydrologic and water quality models: performance measures and evaluation criteria," *Transactions of the ASABE*, vol.58, no.6, pp.1763–1785, 2015. DOI: 10.13031/trans.58.10715.
- [13] D. Yu, P. Xie, X. Dong, X. Hu, J. Liu, Y. Li, T. Peng, H. Ma, K. Wang and S. Xu, "Improvement of the SWAT model for event-based flood simulation on a sub-daily timescale," *Hydrology and Earth System Sciences*, vol.22, no.9, pp.5001–5019, 2018. DOI: 10.5194/hess-22-5001-2018.
- [14] N. Bhagat, "Flood Frequency Analysis Using Gumbel's Distribution Method: A Case Study of Lower Mahi Basin, India," *Journal of Water Resources and Ocean Science*, vol.6, no.4, pp.51–54, 2017. DOI: 10.11648/j.wros.20170604.11.
- [15] B. P. Biedent, C. W. Huber and E. B. Vieux, *Hydrology and floodplain analysis*, 5th edition Pearson, 2012, pp.192-229.
- [16] T. V. Chow, R. D. Maidment and W. L. Mays, *Applied hydrology*, McGraw-Hill, 1988, pp.380-391.
- [17] S. R. Gupta, *Hydrology and Hydraulic Systems*. Long Grove, Illinois: Waveland Press, 2017, pp.430-450.
- [18] K. Komi, J. Neal, A. M. Trigg and B. Diekkrüger, "Modelling of flood hazard extent in data sparse areas: a case study of the Oti River basin, West Africa," *Journal of Hydrology: Regional Studies* vol.10, no.1-2, pp.122–132, 2018. DOI: 10.1016/j.ejrh.2017.03.001.

Biographies



Worapong Lohpaisankrit received his Ph.D. in Civil Engineering from the Technische Universität Braunschweig, Germany, in 2018. He is currently working as a lecturer at the Faculty of Engineering, Khon Kaen University, Thailand. His current research focuses on floods and droughts, river basin modelling and management, and impacts of climate and land use changes on water resources.



Haris Prasanchum received his Ph.D. in Civil Engineering from Mahasarakham University, Thailand in 2017. He is currently an assistant professor at the Department of Civil Engineering, the Faculty of Engineering in Rajamangala University of Technology Isan, Khon Kaen campus, Thailand. His research interests include hydrological processes modelling, impact of climate and land use changes on water resources management, and reservoir engineering.